QUANTIFYING MINERAL ABUNDANCES IN MIXTURES USING RAMAN SPECTROSCOPY: CALCULATING RAMAN COEFFICIENTS USING A DIAMOND REFERENCE. L. B. Breitenfeld[1], M. D. Dyar[1], CJ Carey[2], P. Bartholomew[3], T. J. Tague, Jr.[4], P. Wang[4], S. Mertzmann[5], S. A. Byrne[1], M. C. Crowley, C. Leight[1], and E. Watts[1]. [1]Dept. of Astronomy, Mount Holyoke College, South Hadley, MA 01075, breit22l@mtholyoke.edu, [2]Univ. of Massachusetts Amherst, Amherst MA 01003, [3]Univ. of New Haven, West Haven, CT 06516, [4]Bruker Optics, Inc., Billerica, MA 01821, [4]Franklin and Marshall College, Lancaster, PA, 17603.

Introduction: Over the coming decade, three different Raman instruments will be employed on the surface of Mars (RLS on *ExoMars*, SuperCam and SHERLOC on *Mars 2020*). Although their implementations differ, they share the capability to fingerprint surface minerals and inform Martian geology and geochemistry. Capabilities of these instruments have largely been demonstrated using pure mineral spectra from phases with high Raman cross sections and easily-diagnostic peaks. Only a few studies have evaluated the accuracy with which matching can be done on impure or mixed minerals [1-3]. Many geoscience users employ the CrystalSleuth matching software associated with the rruff.info web site [4], but many minerals there lack XRD phase confirmation and comparisons to data acquired on other instruments may not be appropriate without pre-processing [5] and may lead to reduced matching accuracy.

This project focuses on the interpretation of Raman spectra in mineral mixtures. Quantitative relationships between peak intensity and mineral abundance are obscured by many complicating factors: exciting laser frequency, the Raman cross section of the mineral, crystal orientation, and long-range chemical and structural ordering in the crystal lattices [6]. Even if a broad-spot Raman laser samples multiple grains to average-out crystal orientation, the highly variable Raman cross-sections of minerals [7] confound direct estimation of quantitative mineral abundances from mixtures using Raman spectra. Here, we show that making binary mixtures of pure minerals with a reference (here, diamond) solves the un-mixing problem by allowing determination of Raman Coefficients that relate the areas of mineral peaks to those of a diamond standard. These ratios, which are independent of both laser energy and normalization techniques, permit quantitative estimates of mineral modes to be accurately produced using Raman spectra of mineral mixtures.

Sample Selection and Preparation: Mineral species were chosen to be phases typically found on Mars. Suitable samples were obtained from our own and museum collections and dealers. Each of 23 mineral samples was hand-picked for purity, crushed in a tungsten shatterbox, and sieved to 25-45 μm grain sizes. X-ray diffraction and electron microprobe analysis (EMPA) of each sample were performed at Franklin and Marshall College and Brown University (Joseph Boesenberg, analyst), respectively. These results confirmed sample purity and provided chemical compositions of each phase for calculation of mineral density needed to create mineral mixtures on a volume basis.

Synthetic diamond was chosen as a reference for the Raman Coefficient ratios because it has a simple spectrum with only one strong peak at 1332 cm^{-1} that does not overlap with common rock-forming minerals. The peak is so strong that it dwarfs the Raman features in most rock-forming minerals. A diamond:mineral volume ratio of 5:95 was found to give comparable intensities to diamond and mineral peaks (**Figure 1**), allowing ratios between peak areas to be most accu-

Table 1. Pure samples studied and calculated densities, D

ID	Species	D
Synthetic	Diamond (Eastwind E-DPRVDC030-60)	3.52
ICOSA-1	Alunite, synthetic (Poland)	2.74
ICOSA-2	Anhydrite (Naica, Mexico)	2.97
ICOSA-3	Augite (Harcourt, ON)	3.43
ICOSA-4	Bytownite (Crystal Bay, MN)	2.71
ICOSA-5	Calcite (Rossie, NY)	2.71
ICOSA-6	Clinochlore (Clay Minerals Soc., CCa-2)	2.66
ICOSA-7	Diopside (Hershel, ON)	3.34
ICOSA-8	Enstatite (Tanzania)	3.41
ICOSA-9	Forsterite (San Carlos, AZ)	3.38
ICOSA-10	Gypsum (Niacia, Mexico)	2.30
ICOSA-11	Hematite (Custer Co., SD)	5.30
ICOSA-12	Ilmenite (MHC 711, locality unknown)	4.65
ICOSA-13	Jarosite (Arlington Hwy. 187)	3.09
ICOSA-14	Labradorite (Chihuahua, Mexico)	2.70
ICOSA-15	Rozenite (Mt. Eaton, BBC Canada)	2.22
ICOSA-16	Magnesite (Brumado, Bahia Brazil)	3.00
ICOSA-17	Magnetite (Ishpeming, MI)	5.15
ICOSA-18	Montmorillonite (CMS, SCa-2)	2.01
ICOSA-19	Nontronite (CMS, NAu-2)	2.30
ICOSA-20	Saponite (JB1545, Bumo Creek, AZ)	2.30
ICOSA-21	Siderite (MHC 7976, locality unknown)	3.85
ICOSA-23	Tremolite (Edwards, NY)	3.06
ICOSA-24	Chabazite (Parrsboro, NS)	2.09

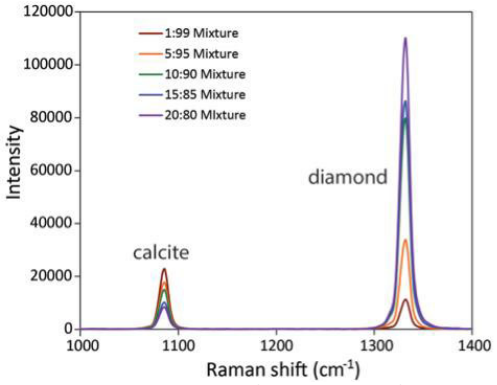

Figure 1. Raman data acquired from mixtures of calcite and diamond in variable volume percentages (e.g., 95 vol% calcite, 5 vol% diamond) on Bruker's BRAVO spectrometer.

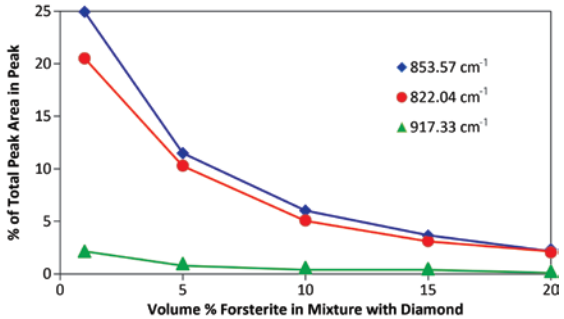

Figure 2. Peak areas for three forsterite peaks at 853.57, 822.04, and 917.33 cm^{-1} (blue, red, and green, respectively) in Raman data acquired from mixtures with diamond in variable volume percentages as indicated, measured on Bruker's BRAVO spectrometer. Data illustrate that peak area is not directly related to mineral abundance due to the variable Raman cross section associated with the bond giving rise to each peak.

rately calculated. The 5:95 mixtures were run on Bruker's BRAVO spectrometer using 758 and 852 nm lasers simultaneously. With a scan time of 10s and wavenumber range of 300-3350 cm^{-1}, each sample was run 3× and the spectra averaged. The BRAVO produces baseline-subtracted data. Finally, diagnostic peaks for each element were fit using Gaussian peaks, and the resultant peak areas were tabulated.

Results: The areas of each mineral species peaks were calculated along with those of the prominent diamond peak. The ratio of those areas is termed a "Raman Coefficient" (R.C.), for each peak that expresses the relationship between peak area in each mineral and its abundance (**Table 2**) in volume mixtures. R.C. values are analogous to molar absorptivity in that peak area is related to molar abundance of each mineral species. R.C. values are needed to obtain quantitative estimates of species abundances because peak area does not vary linearly with volume fraction (**Figure 2**) for any peak in any mixture of minerals we tested.

Discussion: Samples are listed in Table 2 in order of R.C. from smallest to largest. Mineralogical groupings are apparent. Silicates have very low R.C.'s. All R.C. values above 0.24 are non-silicates, with an oxide (ilmenite) being the highest. These trends show quantitatively the effect of mineral structure on bond polarizability and in turn on Raman cross-section. Further data acquisition of these standards and other minerals in 95:5 mixtures with diamond will establish the variability of R.C.'s over varying instrumentation, sample types, and analytical conditions.

Implications: Peak intensities in Raman spectroscopy are affected by laser frequency, Raman cross section, orientation, cation ordering in the minerals, and many experimental factors [6]. The Raman coefficeints calculated here are an empirical formulation that reflects all these factors and provides a simple relationship between peak area and species abundance in mixtures. These data will form a basis for simple calculations of mineral abundances in mixtures of powdered phases, and lay the groundwork for both theoretical (e.g., Hapke-analog) and machne learning algorithms for unmixing.

Acknowledgements: Funded by NASA NNA14AB04A and the Massachusetts Space Grant Consortium.

References: [1] Bartholomew P. R. (2013) *Geostand. & Geoanal. Res.*, 37, 353-359. [2] Lopez-Reyes G. et al. (2014) *Amer. Mineral.*, 99, 1570-1579. [3] Clegg S.M. et al. (2014) *Appl. Spectros.*, 68, 925-936. [4] Carey CJ et al. (2015) *J. Raman Spectr.*, 46, 894-903. [5] Ishikawa S.T. and Gulick V.C. (2013) *Comp.Geosci.*, 54, 259–268. [6] Haskin L. A. et al. (1997) *JGR*, 102(E8), 19293–19306. [7] Bartholomew P.R. et al. (2015) *J. Raman Spectrosc.*, 46, 889-893.

Table 2. Raman coefficients (R.C.) at given wavenumbers for pure minerals.

	Strongest Peak		2nd Strongest		3rd Strongest	
Mineral, Formula	**R.C.**	**σ cm^{-1}**	**R.C.**	**σ cm^{-1}**	**R. C.**	**σ cm^{-1}**
Montmorillonite, $(Na,Ca)_{0.3}(Al,Mg)_2Si_4O_{10}(OH)_2 \cdot nH_2O$	0.03	706	0.03	358	n.a.	n.a.
Nontronite, $Na_{0.3}Fe^{3+}{}_2(Si,Al)_4O_{10}(OH)_2 \cdot n(H_2O)$	0.03	608	0.03	432	0.02	690
Rozenite, $Fe^{2+}SO_4 \cdot 4(H_2O)$	0.06	1026	0.03	988	n.a.	n.a.
Labradorite, $(Ca,Na)(Si,Al)_4O_8$	0.07	508	0.01	562	n.a.	n.a.
Saponite, $(Ca,Na)_{0.3}(Mg,Fe^{2+})_3(Si,Al)_4O_{10}(OH)_2 \cdot 4(H_2O)$	0.08	680	0.02	358	n.a.	n.a.
Clinochlore, $(Mg,Fe^{2+})_5Al(Si3Al)O_{10}(OH)_8$	0.08	682	0.03	552	0.01	358
Enstatite, $Mg_2Si_2O_6$	0.09	686	0.03	340	0.03	1008
Forsterite, Mg_2SiO_4	0.10	822	0.09	854	0.01	960
Bytownite, $(Ca,Na)(Si,Al)_4O_8$	0.10	506	n.a.	n.a.	n.a.	n.a.
Augite, $(Ca,Na)(Mg,Fe,Al,Ti)(Si,Al)_2O_6$	0.10	666	0.07	1014	0.03	386
Jarosite, $KFe^{3+}(SO_4)_2(OH)_6$	0.10	1112	0.09	1010	0.05	1148
Chabazite, $(Ca_{0.5},Na,K)_4[Al_4Si_8O_{24}] \cdot 12H_2O$	0.13	466	n.a.	n.a.	n.a.	n.a.
Magnetite, Fe_3O_4	0.14	498	0.09	680	n.a.	n.a.
Diopside, $CaMgSi_2O_6$	0.15	668	0.07	1012	n.a.	n.a.
Tremolite, $Ca_2Mg_5Si_8O_{22}(OH)_2$	0.24	596	0.14	420	0.12	804
Alunite, $KAl_3(SO_4)_2(OH)_6$	0.27	992	0.10	456	0.08	618
Gypsum, $CaSO_4 \cdot 2(H_2O)$	0.36	1008	0.08	1134	0.08	494
Calcite, $CaCO_3$	0.43	1086	0.07	712	0.03	1434
Hematite, Fe_2O_3	0.43	410	0.24	610	0.23	496
Anhydrite, $CaSO_4$	0.53	1016	0.12	498	0.10	1128
Siderite, $Fe^{2+}CO_3$	1.04	1086	n.a.	n.a.	n.a.	n.a.
Magnesite, $MgCO_3$	1.23	1575	0.54	1096	0.26	330
Ilmenite, $Fe^{2+}TiO_3$	1.32	686	n.a.	n.a.	n.a.	n.a.